Thermal Properties and Morphology of Isotactic Polypropylene/Acrylonitrile–Butadiene Rubber Blends in the Presence and Absence of a Nanoclay

Mohammad Razavi-Nouri, Ghasem Naderi, Ali Parvin, Mir Hamid Reza Ghoreishy

Iran Polymer and Petrochemical Institute, P.O. Box 14965-115, Tehran, Iran

Received 29 November 2009; accepted 27 September 2010
DOI 10.1002/app.33752
Published online 3 March 2011 in Wiley Online Library (wileyonlinelibrary.com).

ABSTRACT: A thermoplastic elastomer (TPE) nanocomposite based on polypropylene (PP), acrylonitrile–butadiene rubber (NBR), and a nanoclay (NC) was prepared in a laboratory mixer with a 54/40/6 weight ratio. The effects of NC on the thermal properties, crystalline structure, and phase morphology of the TPE nanocomposite were studied in this work. The results obtained from the nonisothermal crystallization of PP, PP/NBR, and PP/NBR/NC, which was carried out with differential scanning calorimetry, revealed that the overall rate of crystallization of PP decreased with the addition of NBR to PP and increased when NC was incorporated into the nanocomposite. In addition, the crystallite size distribution was more uniform for the PP phase crystallized in the nanocomposite versus the PP itself. Also, although the PP in the reference blend (PP/NBR) crystallized only in the α form, the crystalline structure of the PP incorporated into the nanocomposite was a mixture of α- and γ-crystalline forms. The effects of NC on the phase morphology of PP/NBR blends prepared with three different cooling methods (quenching in liquid nitrogen, cooling between two metal plates at room temperature, and molding at a high temperature in a hot press) were studied. For the samples quenched in liquid nitrogen or cooled between metal plates, a particulate–cocontinuous morphology formed. However, for the samples prepared under a hot press, a laminar-like morphology was observed. In all three cases, a similar particulate–cocontinuous morphology formed for the reference blend, but the rubber inclusions were always smaller than those of the TPE nanocomposite. © 2011 Wiley Periodicals, Inc. J Appl Polym Sci 121: 1365–1371, 2011

Key words: blends; differential scanning calorimetry (DSC); morphology; nanocomposites; poly(propylene) (PP)

INTRODUCTION

Polymer nanocomposites can be regarded as a new category of materials in which nanosized fillers, that is, particles with at least one dimension in the nanometer range [e.g., a nanoclay (NC) or a layered silicate and carbon nanotube], are dispersed into a polymer. The dispersion of NC particles into many polymers is not easily achieved because not only do the particles prefer to stack as agglomerated tactoids but also there is no compatibility between hydrophobic plastics and hydrophilic particles. There are several methods (*in situ* polymerization and solution and melt mixing) for the incorporation of NC into different polymers.[1–3]

Thermoplastic elastomers (TPEs) have received enormous attention for their use in many areas, such as the electrical and automotive industries and medicine, during the past few decades. These materials can be simply processed as thermoplastics materials, but many of their properties are similar to those of rubbers.[4] TPEs are rubber blends with a crystallizable thermoplastic polymer or a synthesized block copolymer.[5] The mechanical properties of TPEs depend both on the properties of the constituents and the phase morphology of the resultant blends. The final morphology of the blends is mainly controlled by several factors, such as the concentration of each polymer, the viscosity ratio, the processing conditions, the elasticity ratio, and the interfacial tension between the components.[6,7]

Acrylonitrile–butadiene rubber (NBR) is a good, oil-resistant elastomer, but its electrical-insulation properties and especially its ozone resistance are relatively low. To improve the overall properties of NBR, it can be blended with plastics such as polypropylene (PP). PP belongs to the polyolefin family of polymers and has relatively well-balanced physical and mechanical properties as well as excellent processability and a low cost. Therefore, the combination of these two polymers should provide a material with good flexibility, excellent oil resistance, and easy processability. However, these materials are incompatible in nature, and the physical and chemical interactions of these two polymers are poor at the interphases of the polymers in

Correspondence to: M. Razavi-Nouri (m.razavi@ippi.ac.ir).

their blends. Therefore, a compatibilizer is required to improve the properties of PP/NBR blends.[8–11] Coran and Patel[12–14] conducted many studies on the production of PP–NBR block copolymers and the manufacture of suitable block copolymers in internal mixers during melt blending.

Chung and Coran[15] also studied the morphology of several plastic/rubber blends with different polarities during molten-state mixing, compression molding, and cold pressing. For a 60/40 PP/ethylene–propylene–diene monomer (EPDM) blend, they found that after 4 min of molten-state mixing, it had a mixed, particulate–cocontinuous morphology. This morphology changed to a laminar structure after cold pressing and became random and cocontinuous because of coalescence after compression molding. In addition, a finer phase morphology was formed when the polarities of the components were nearly matched; however, when the polarities were mismatched, the morphology with the greatest amount of coarsening was formed during compression molding. Moreover, they found that the effect of the interfacial tension or polarity match on the particle size of the polymer blends was more dominant than the viscosity ratio of the polymers.

In this article, we report on the influence of an NC on the crystallization and phase morphology of uncompatibilized PP/NBR blends prepared with three different cooling methods. Because our purpose was to observe only the effects of NC on the blend morphology, we did not add any material as a compatibilizer to the blends. This, of course, will be studied in our future work.

EXPERIMENTAL

Materials

Isotactic PP (PP 500P) (Yanbu, Saudi Arabia) was supplied by Sabic Co. (Saudi Arabia) with a melt flow index of 3 g/10 min (190°C and 2.160 kg) and a density of 900 kg/m^3. NBR (Europrene N 3345) with an acrylonitrile content of 33%, a density of 990 kg/m^3, and a Mooney viscosity of 45 [ML(1 + 4) at 100°C] was supplied by Polimeri Europa Co. (Ferrara, Italy). NC (Cloisite 15A) was obtained from Southern Clay Products (Gonzales, Texas, United States) with a specific gravity of 1.66; it was a natural montmorillonite modified with dimethyl dehydrogenated tallow quaternary ammonium with a cation-exchange capacity of 125 mequiv/100 g.

Blend preparation

NC was dried at 100°C for 24 h in a vacuum oven before it was mixed with other ingredients. For the preparation of the TPE nanocomposites, a two-step mixing procedure was employed. To prepare a master batch of PP and Cloisite 15A, the two components were first melt-blended in an internal mixer (HBI SYS 90 Rheomix, Haake) (Karlsruhe, Germany) equipped with a pair of roller blades at 190°C and 100 rpm for 10 min. The prepared master batch was then chopped into small pieces and introduced into the same mixer at the same temperature and rotor speed. After 2 min, when the PP was completely melted and the torque had leveled off, the appropriate weight of NBR was added, and mixing was continued for another 5 min to produce a PP/NBR/NC TPE nanocomposite (54/40/6 by weight). For comparison, a reference PP/NBR blend with a weight ratio of 60/40 was also prepared. For the scanning electron microscopy (SEM) examination of the nanocomposite and the PP/NBR blend, the hot blends were immediately cooled in different ways after their removal from the mixer. The mixtures were quenched in liquid nitrogen, were pressed between two metal plates at room temperature, or were placed between two plates of a Toyoseiki mini test hydraulic press (Tokyo, Japan) under pressure at 190°C for 6 min and then cooled with water while they remained under the press.

Transmission electron microscopy (TEM)

Ultrathin sections of the TPE nanocomposite were prepared: the specimen was mounted in an epoxy (Araldite) resin and cut with a diamond knife at −50°C with a Reichert OMUw ultramicrotome (Vienna, Austria). The thickness of the sample was approximately 80 nm. Then, the ultrathin sections were examined with a Philips CM-200 transmission electron microscope (Eindhoven, The Netherlands) operated at an accelerating voltage of 120 kV.

Differential scanning calorimetry (DSC)

Thermal analysis was carried out with a PerkinElmer Pyris I differential scanning calorimeter (Waltham, Massachusetts, United States) interfaced to a personal computer. The temperature scale of the calorimeter was calibrated with indium. All samples were weighed (5 ± 0.2 mg) and enclosed in an aluminum pan. An empty aluminum pan was also used as a reference. The samples were first heated to 200°C and kept at this temperature for 5 min. After this period, each sample was cooled at the cooling rate of 10 K/min to 25°C. The samples were kept at this temperature for another 5 min and heated again to 200°C at the heating rate of 10 K/min. All the thermal experiments were carried out under a constant flow of nitrogen to prevent any possible degradation.

X-ray diffractometry

The X-ray diffraction patterns of the NC and the nanocomposite were obtained at a low 2θ angle with

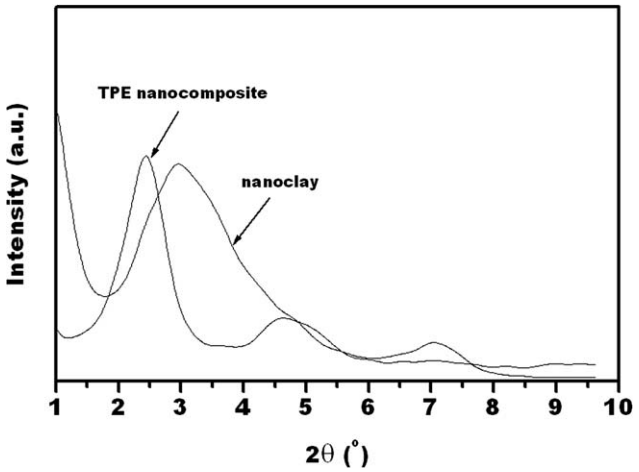

Figure 1 X-ray diffraction patterns of Cloisite 15A and the TPE nanocomposite.

a Philips X'Pert instrument operated with Cu Kα radiation (wavelength = 1.54 Å) at 40 kV and 40 mA. The crystalline structures of PP in the reference blend and the TPE nanocomposite were also studied with the same instrument, but the 2θ values ranged from 10 to 30° in steps of 1°/min, and the count time was 1 s/step. All the samples except for NC were cut from 2-mm-thick compression-molded sheets.

SEM

A Vega II XMU scanning electron microscope (Brno, Czech Republic) was used to observe the fracture surfaces of the materials prepared under different cooling conditions. The samples were first fractured in half at the temperature of liquid nitrogen, and the fracture surfaces were then treated with acetone to etch out the rubber component. The treated samples were mounted onto a metal stub, and the fracture surfaces were sputtered with gold.

RESULTS AND DISCUSSION

X-ray diffraction pattern analysis

The X-ray diffraction patterns of the NC and the TPE nanocomposite are shown in Figure 1. The reflection corresponding to the (001) plane of Cloisite 15A can be observed at 2θ = 2.91° before its mixing with PP and NBR. This is equal to the distance of 30.32 Å between the adjacent planes. However, for NC incorporated into the 54/40/6 nanocomposite, the reflection can be seen at 2θ = 2.43°, which corresponds to an interlayer spacing of 36.31 Å. The shift of the (001) plane of NC to lower 2θ values after its mixing with PP and NBR agrees with the fact that Cloisite 15A should have an intercalated structure in the TPE nanocomposite.

PP has three main well-defined crystallographic phases: a monoclinic (α) form, a hexagonal (β) form, and a triclinic (γ) form.[16–19] The X-ray patterns of the PP/NBR blend and the PP/NBR/NC nanocomposite are shown in Figure 2. Both patterns have several sharp diffraction lines superimposed on a broad, amorphous background. α-PP reflections are present at 2θ values of 14.15, 16.90, 18.56, 21.18, and 21.85°. These lines are related to the (110), (040), (130), (111), (131), and (041) lattice planes. The diffraction line at 21.85° corresponds to both the (131) and (041) planes.[20] The diffraction lines attributed to the β and γ forms appear at 2θ values of approximately 15–16 and 20°, respectively. As Figure 2 shows, although PP in the PP/NBR blend was crystallized only in the α form, a mixture of α- and γ-crystalline structures was present for the PP crystallized in the PP/NBR/NC nanocomposite. This shows that the incorporation of NC into PP facilitated the production of the γ-form structure, which was less stable than the α form. The fractional amount of the γ-crystalline form was estimated with $I_\gamma/(I_\alpha + I_\gamma)$ "I_α" is the intensity of α-phase at 2θ=18.6° and "Iy" is the intensity of γ-phase at 2θ=20° (see Figure 2).[21] Approximately 8% of the total crystalline structure was the γ-crystalline form.

TEM images of the nanocomposite

TEM images of the nanocomposite were taken to obtain better insight into the NC dispersion into the matrix, as shown in Figure 3. The three materials are shown with different arrows. Because the density of PP is lower than that of NBR, it appears in a brighter color than the NBR phase. The silicate layers can also be seen as black lines. Moreover, the silicate layers were mainly dispersed in the PP

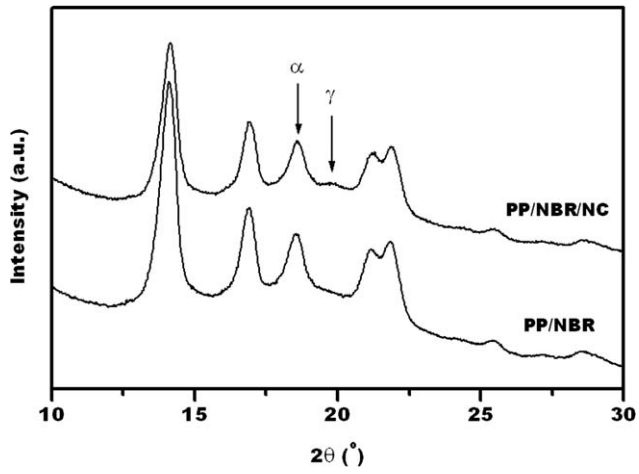

Figure 2 Wide-angle X-ray diffraction spectra of the PP/NBR blend and the PP/NBR/NC nanocomposite.

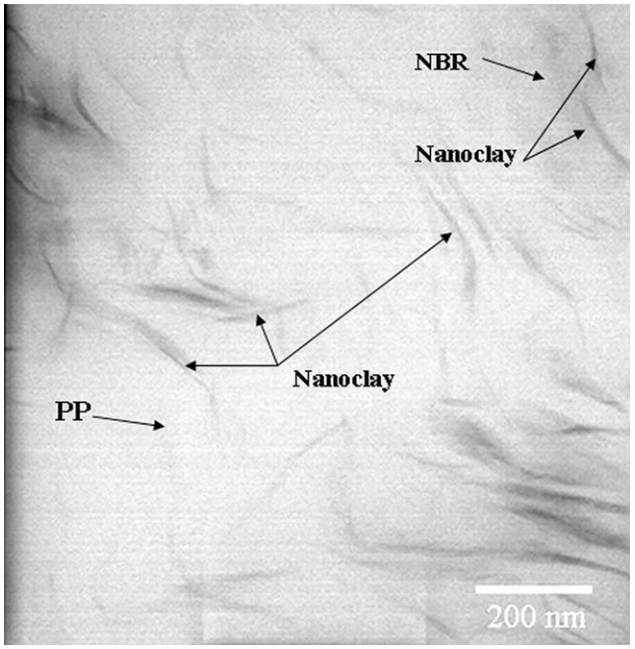

Figure 3 TEM image of the TPE nanocomposite.

matrix, but a small amount of NC penetrated the NBR phase as well. It is also clear from the figure that a significant fraction of the silicate layers were either intercalated or exfoliated in the two phases, whereas a small amount remained in the form of a more clustered state.

Thermal analysis

The DSC crystallization exotherms of PP, NBR/PP, and NBR/PP/NC from the molten state at the cooling rate of 10 K/min are depicted in Figure 4. Some useful parameters were obtained from Figure 4. Their definitions are as follows.[22] T_{onset} is the high-temperature side of the exotherm and the temperature at the intercept of the tangents at the baseline. T_p is the peak temperature of the crystallization

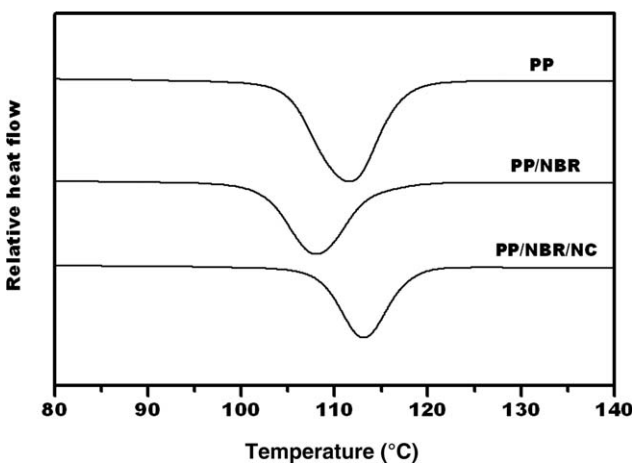

Figure 4 DSC nonisothermal crystallization exotherms of PP, PP/NBR, and the PP/NBR/NC nanocomposite.

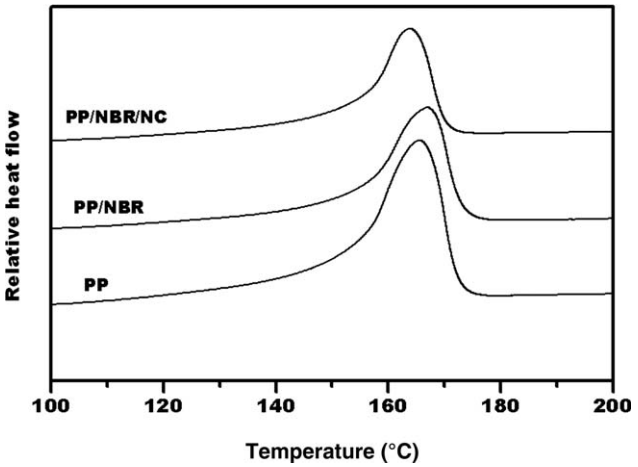

Figure 5 Melting endotherms of PP, PP/NBR, and the PP/NBR/NC nanocomposite.

exotherm, and $T_{onset} - T_p$ is inversely related to the general rate of crystallization. Δw_c is the width at half-height of the crystallization peak and is directly related to the crystallite size distribution. S_i is the slope of the initial linear section of the exotherm, which is associated with the rate of nucleation. The enthalpy of melting (ΔH_f), the melting temperature at the peak (T_m), and the width at half-height of the melting peak (Δw_m) were all determined from the DSC melting endotherms (Fig. 5). The degree of crystallinity (X_c) was also calculated with the following equation[23]:

$$X_c = \frac{\Delta H_f}{(1 - \phi)\Delta H_f^o} \quad (1)$$

where ΔH_f^o is the theoretical enthalpy of 100% crystalline PP (considered to be 209 J/g) and $1 - \varphi$ is the weight fraction of PP.[24] All the calculated nonisothermal parameters are summarized in Table I. The T_{onset} and T_p values for the PP/NBR blend were lower than those for PP. This could be attributed to NBR, which prevented PP crystallization by shifting T_{onset} and T_p to lower temperatures. However, both temperatures were higher for the TPE nanocomposite versus PP. This could be related to the heterogeneous nucleation effect of the NC particles, which made the crystallization of PP much easier when it was cooled from a temperature higher than its melting temperature. $T_m - T_p$, can be a measure used for the evaluation of the crystallization behavior of polymers. This value was lower for the nanocomposite versus PP, and this showed that the induction time for the crystallization of PP for the PP/NBR/NC TPE was lower than that for the pristine polymer. The decrease in the value of $T_{onset} - T_p$ was also consistent with the accelerated rate of crystallization of the polymer.[25,26] Therefore, the increase and decrease of these two parameters for the PP/

TABLE I
Various Parameters Determined from Nonisothermal Crystallization Exotherms and Melting Endotherms of PP, PP/NBR, and PP/NBR/NC

Sample	T_p (°C)	ΔH_f (J/g)	X_c (%)	T_{onset} (°C)	$T_{onset} - T_p$ (°C)	Δw_c	S_i	T_m (°C)	$T_m - T_p$ (°C)	Δw_m
PP	111.6	77.2	37	117.7	6.1	7.8	4.9	165.7	54.1	12.3
PP/NBR	108.0	48.9	39	114.4	6.4	7.3	3.3	166.9	58.9	11.1
PP/NBR/NC	113.1	44.6	40	118.5	5.4	5.8	4.4	163.8	50.7	9.6

NBR blend and the PP/NBR/NC nanocomposite, respectively, indicated that the overall rate of crystallization of PP decreased when NBR was added to PP and increased when NC was introduced into the PP phase of the nanocomposite. It was also observed that S_i for the nanocomposite was slightly lower than S_i for PP but was higher than that for the PP/NBR blend. It could be inferred that the rate of nucleation was highest for the pristine polymer and lowest for the reference blend. Both Δw_c and Δw_m were lowest for the nanocomposite versus PP and the PP/NBR blend. This implied that the crystallite size distribution was more uniform for the PP incorporated into the nanocomposite than for the pristine polymer. The results also showed that the degree of crystallization only slightly changed for PP/NBR and PP/NBR/NC in comparison with PP itself.

Morphology

Figure 6(a,b) shows SEM micrographs of the PP/NBR blend and the PP/NBR/NC nanocomposite, respectively, after they were quenched in liquid nitrogen. The rubber particles, which were removed by selective etching of the materials in acetone, can be observed as dark holes. In both cases, the tendency was toward the formation of a mixed particulate–cocontinuous morphology. A comparison of Figure 6(a,b) reveals that the size of the rubber droplets increased with the addition of NC to the nanocomposite.

The SEM micrographs of the PP/NBR blend and the PP/NBR/NC nanocomposite that were cooled by pressing between two metal plates at room temperature are shown in Figure 7(a,b), respectively. As can be seen in Figure 7(a), the rubber droplets were generally larger and more elongated than those appearing in Figure 6(a). As can be seen in Figure 7(b), the incorporation of NC into the nanocomposite changed the morphology toward a laminar-like morphology with the presence of highly elongated rubber inclusions. This was similar to what Chung and Coran[15] reported for an EPDM/PP blend with no other ingredients.

Figure 8(a,b) shows the SEM micrographs of the PP/NBR blend and the PP/NBR/NC nanocomposite, respectively, after they were compression-molded in a hot press. Figure 8(a) shows that the rubber droplets were larger than those of the PP/NBR blend quenched in liquid nitrogen [Fig. 6(a)] or cooled between two plates [Fig. 7(a)] because of the

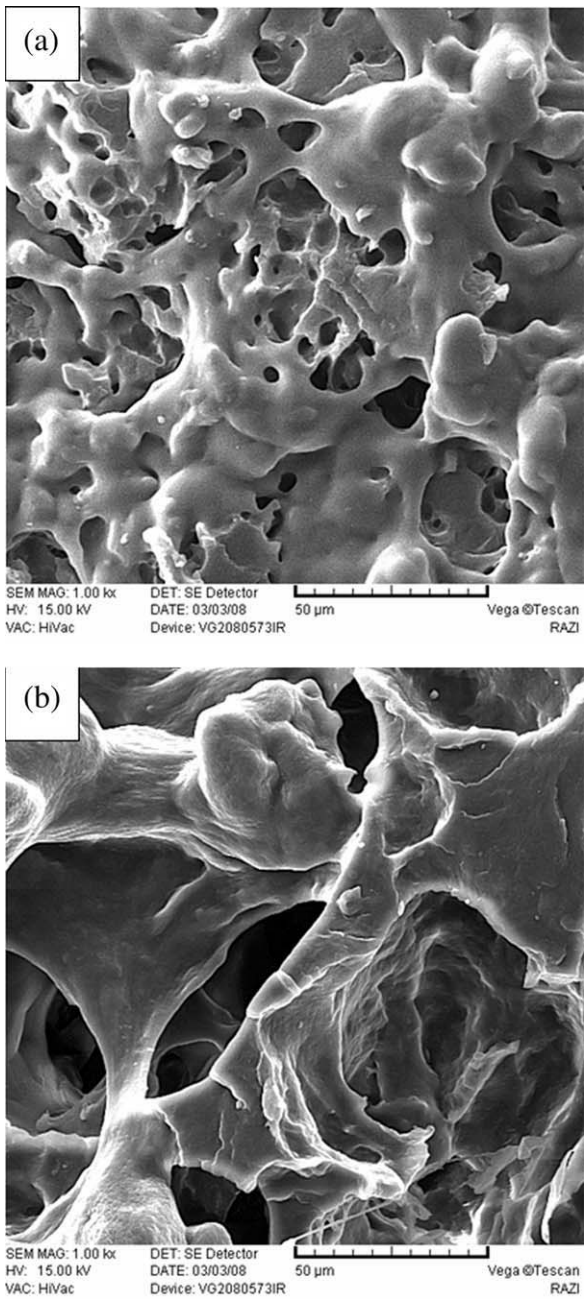

Figure 6 SEM micrographs of (a) the PP/NBR blend and (b) the PP/NBR/NC nanocomposite after they were quenched in liquid nitrogen.

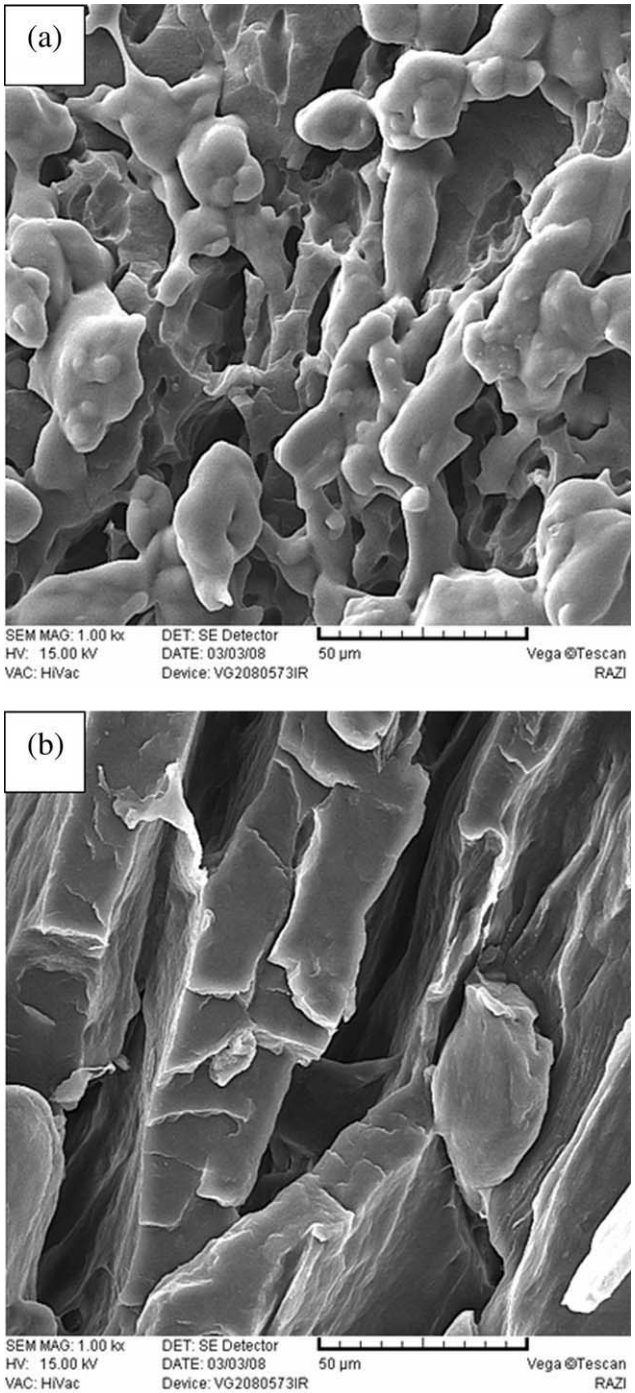

Figure 7 SEM micrographs of (a) the PP/NBR blend and (b) the PP/NBR/NC nanocomposite after they were cooled between two metal plates at room temperature.

coalescence of the particles at a high temperature. In this situation, molding at 190°C helped the polymers to coalescence and form larger inclusions. Figure 8(b) also reveals that the morphology was again similar to a mixed particulate–cocontinuous morphology, and the addition of NC made the rubber droplets larger in the nanocomposite than the reference blend.

Naderi et al.[27] studied the effect of NC on the particle size of vulcanized rubber dispersed throughout the matrix in thermoplastic, vulcanized PP/EPDM nanocomposites. They found that NC could play an important role in determining the sample morphology, and the size of the vulcanized rubber particles dispersed throughout the PP matrix increased with the incorporation of NC in comparison with the particles without NC. This was attributed to the effect of tetramethyl thiuram disulfide, which made

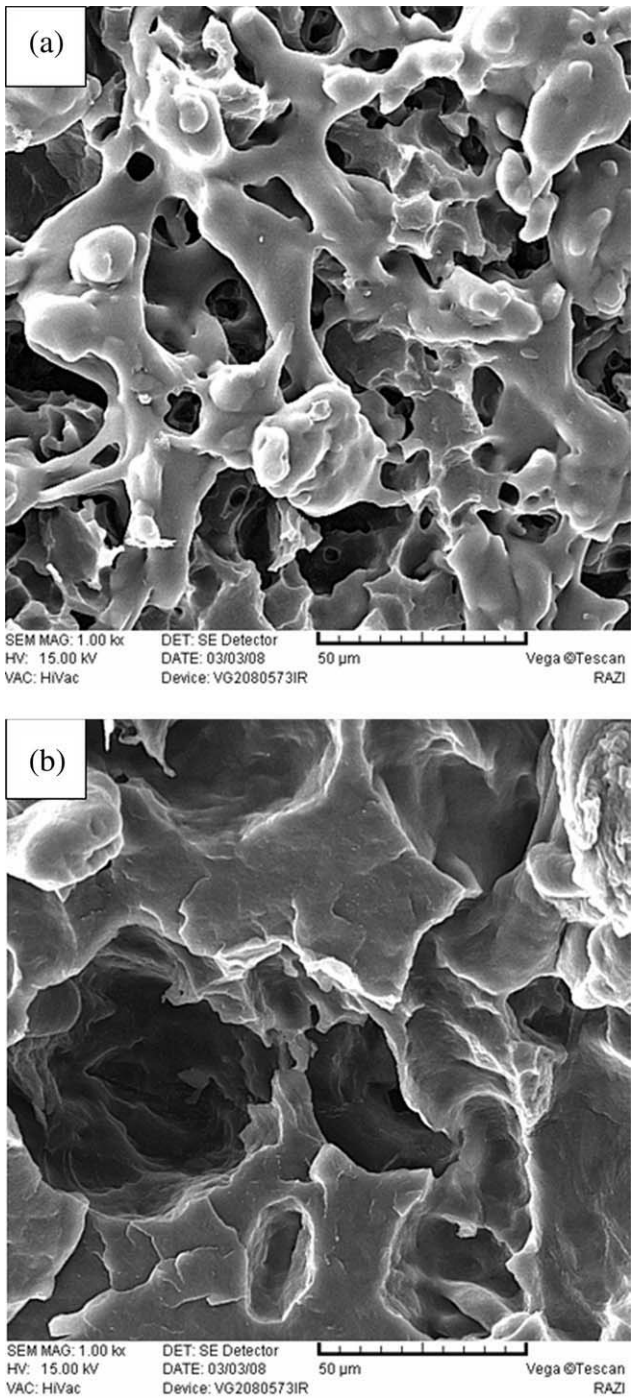

Figure 8 SEM micrographs of (a) the PP/NBR blend and (b) the PP/NBR/NC nanocomposite after they were melted and cooled under a press.

the rubber phase more polar and, therefore, caused some of the NC particles to immigrate into the rubber phase before the curing cycle was completed. This could change the viscosity ratio of the two materials, so the size of the rubber phase increased. Yoo et al.[28] investigated the effect of NC on the morphology of an amorphous polyamide/ethylene 1-octene (EOR) copolymer nanocomposite prepared via melt processing. They found that the EOR particles were well dispersed throughout the matrix with a much smaller size, and the shape of the EOR phase was also more irregular in comparison with that of an amorphous polyamide/EOR blend. These two changes in the size and regularity of the EOR phase were related to two competing effects of the viscosity buildup of the matrix due to the incorporation of NC and also to barrier effects of NC on the coalescence of rubber particles. They reported that the barrier effect was the more effective mechanism in reducing the size of EOR particles.

We have inferred from our results that the effect of the viscosity ratio on the studied nanocomposite is more dominant than the barrier effect in the development of the morphology. This is similar to what Naderi et al.[27] earlier reported for a vulcanized PP/EPDM system.

CONCLUSIONS

The influence of NC on the thermal and crystalline structure as well as the phase morphology of the PP/NBR/NC nanocomposite was compared with its influence on the PP/NBR blend. The results of nonisothermal crystallization studies showed that the overall rate of crystallization was highest and the crystallite size distribution was narrowest for PP incorporated into the nanocomposite in comparison with the other studied materials. It was also found that the rate of nucleation decreased when NBR was added to PP and increased again when NC was incorporated into PP in the nanocomposite, but it still remained less than that of PP itself. An investigation of the effect of NC on the phase morphology of PP/NBR blends prepared with three different methods revealed that although a particulate–cocontinuous morphology formed for the samples quenched in liquid nitrogen or prepared under a hot press, a laminar-like morphology with elongated rubber inclusions was observed for the samples cooled between metal plates. The morphology of the reference blend remained particulate–cocontinuous; the rubber droplets were always smaller than those of the samples containing NC with all the preparation methods employed. This could imply that for the studied nanocomposite, the change in the viscosity ratio due to the incorporation of NC in both phases was a more powerful factor in changing the morphology than the barrier effect.

References

1. Paul, D. R.; Robeson, L. M. Polymer 2008, 49, 3187.
2. Pavlidou, S.; Papaspyrides, C. D. Prog Polym Sci 2008, 33, 1119.
3. He, J.-D.; Cheung, M. K.; Yang, M.-S.; Qi, Z. J Appl Polym Sci 2003, 89, 3404.
4. Handbook of Elastomers—New Developments and Technology; Bhowmick, A. K., Stephens, H. L., Eds.; Marcel Dekker: New York, 1988.
5. Joseph, A.; George, S.; Joseph, K.; Thomas, S. J Appl Polym Sci 2006, 102, 2067.
6. Naderi, G.; Lafleur, P. G.; Dubois, C. Polym Compos 2008, 29, 1301.
7. Naderi, G.; Razavi-Nouri, M.; Mehrabzadeh, M.; Bakhshandeh, G. Iran Polym J 1999, 8, 37.
8. Zhang, X.; Huang, H.; Zhang, Y. J Appl Polym Sci 2002, 85, 2862.
9. George, S.; Varughese, K. T.; Thomas, S. Polymer 2000, 41, 5485.
10. George, S.; Varughese, K. T.; Thomas, S. Polymer 2000, 41, 579.
11. George, S.; Neelakantan, N. R.; Varughese, K. T.; Thomas, S. J Polym Sci Part B: Polym Phys 1997, 35, 2309.
12. Coran, A. Y.; Patel, R. Rubber Chem Technol 1983, 56, 1045.
13. Coran, A. Y.; Patel, R. U.S. Pat. 4,355,139 (1982).
14. Coran, A. Y.; Patel, R. U.S. Pat. 4,409,365 (1983).
15. Chung, O.; Coran, A. Y. Rubber Chem Technol 1997, 70, 781.
16. Beckett, D. R.; Chalmers, J. M.; Mackenzie, M. W.; Willis, H. A.; Edwards, H. G. M.; Lees, J. S.; Long, D. A. Eur Polym J 1985, 21, 849.
17. Caldas, V.; Brown, G. R.; Nohr, R. S.; MacDonald, J. G.; Raboin, L. E. Polymer 1994, 35, 899.
18. Thomann, R.; Kressler, J.; Setz, S.; Wang, C.; Mülhaupt, R. Polymer 1996, 37, 2627.
19. Naiki, M.; Kikkawa, T.; Endo, Y.; Nozaki, K.; Yamamoto, T.; Hara, T. Polymer 2001, 42, 5471.
20. Turner-Jones, A.; Cobbold, A. J. Polym Sci Part B: Polym Lett 1968, 6, 539.
21. Pae, K. D. J Polym Sci Part A2: Polym Phys 1968, 6, 657.
22. Razavi-Nouri, M.; Ghorbanzadeh-Ahangari, M.; Fereidoon, A.; Jahanshahi, A. Polym Test 2009, 28, 46.
23. Tjong, S. C.; Bao, S. P. J Polym Sci Part B: Polym Phys 2005, 43, 253.
24. Chen, M.; Tian, G.; Zhang, Y.; Wan, C.; Zhang, Y. J Appl Polym Sci 2006, 100, 1889.
25. Zhou, Z.; Wang, S.; Zhang, Y.; Zhang, Y. J Appl Polym Sci 2006, 102, 4823.
26. Li, Y.; Wang, S.; Zhang, Y.; Zhang, Y. J Appl Polym Sci 2006, 102, 104.
27. Naderi, G.; Lafleur, P. G.; Dubois, C. Polym Eng Sci 2007, 47, 207.
28. Yoo, Y.; Cui, L.; Yoon, P. J.; Paul, D. R. Macromolecules 2010, 43, 615.